

Connective Tissue in Squid Mantle Is Arranged to Accommodate Strain Gradients

JESSICA A. KURTH^{1,*}, JOSEPH T. THOMPSON², AND WILLIAM M. KIER¹

¹*Department of Biology, University of North Carolina at Chapel Hill, Chapel Hill, North Carolina 27599; and* ²*Department of Biology, Franklin & Marshall College, Lancaster, Pennsylvania 17603*

*The hollow, cylindrical shape of many soft-bodied animals results in nonuniform circumferential strain across the muscular body wall as the body diameter changes. This could complicate reinforcement with connective tissue because fibers in one region of the body wall must accommodate greater strain than those in other regions. We investigated this issue in the mantle of the squid *Doryteuthis pealeii*. During escape jet locomotion, the decrease in diameter during the jet requires circumferential strain at the inner surface of the mantle wall to be 1.5 times greater than that at the outer surface of the mantle wall, with a continuous gradient of strain between the two surfaces. We predicted that, to accommodate the greater strain, the intramuscular collagen fibers near the inner surface would either be arranged in a different manner or would have different mechanical properties from fibers near the outer surface. We observed a different arrangement: when the mantle was contracted, fibers from near the inner surface of the mantle wall were significantly more folded than the fibers along the outer surface. When the mantle was fully expanded radially, all of the fibers straightened almost completely, with no significant difference in folding between the inner and outer fibers. The modification of the connective tissue network in the mantle in response to a nonuniform distribution of strain may not be limited to squid, but may be important in other soft-bodied invertebrates and in the walls of blood vessels.*

Hollow, cylindrical muscular organs and bodies are widespread in animals and are used for movement, locomotion, burrowing, and pumping, with support provided by a hydrostatic skeleton (1, 2). The muscular walls typically lack

compressible gas-filled spaces (but see 3), and the tissues are thus essentially constant in volume so that the wall thickness changes when the diameter changes; the magnitude of the thickness change depends on the extent of both diameter change and any simultaneous length change. This change in wall thickness means that when these cylindrical muscular organs change diameter, the circumferential strain (strain is typically defined as the change in length divided by the original length) near the inner surface can be significantly greater than that near the outer surface (4, 5) (Fig. 1A).

A nonuniform distribution of circumferential strain has implications for muscle function and also poses challenges for the connective tissue fibers that play critical roles in controlling deformation. Specifically, collagen fiber networks in one region of the body wall may need to accommodate significantly greater strain during locomotion and movement than in other regions. Given the stiffness and limited extensibility of collagen, how are the organization and material properties of collagen fiber networks altered to accommodate these differences in circumferential strain? We investigated aspects of this question in connective tissue fibers in the mantle of squid.

The mantle of squid contains distinct networks of intramuscular collagen fibers. We focused on the fibers in a network termed Intramuscular Fiber System 3 (IM-3); the fibers run circumferentially around the mantle, parallel to the circular muscle fibers that provide power for jet propulsion and ventilation of the mantle cavity (6, 7) (Fig. 1B, C). These fibers appear crimped or wavy in a resting or contracted mantle and are thought to provide an upper limit to mantle expansion (8). They have also been implicated in elastic energy storage during certain patterns of respiration and especially during “hyper-inflation” (expansion of the

Received 10 March 2014; accepted 23 June 2014.

* To whom correspondence should be addressed. E-mail: jkurth@live.unc.edu

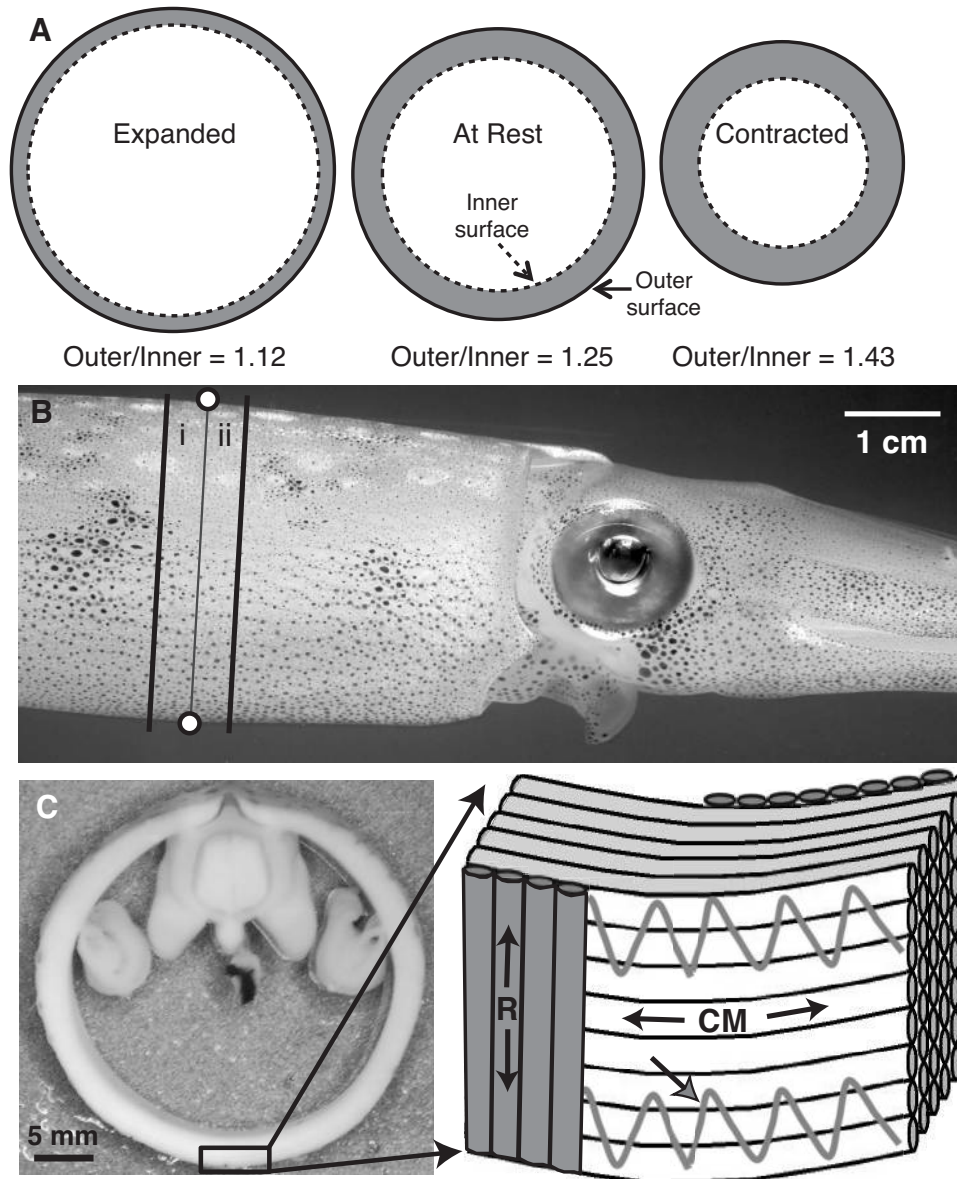


Figure 1. (A) Cross section through a cylinder of constant length with an isovolumetric body wall (gray). In the cylinder at rest, the ratio of the outer to inner surface lengths is 1.25. As the body wall expands or contracts radially, the ratio changes because the inner surface of the body wall experiences proportionately greater changes in circumference, and therefore circumferential strain, than the outer surface for a given contraction or expansion. (B) An adult individual of *Doryteuthis pealeii* illustrating the locations of the sonomicrometry crystals (white circles) and the two tissue rings (i, ii). (C) Ring of mantle tissue and schematic illustrating the radial (R) and circular (CM) muscle fibers and the IM-3 fibers (gray arrowhead). The schematic is not to scale, and other intramuscular collagen fiber systems are not shown.

mantle beyond the resting state) immediately preceding the powerful escape jet (9).

To serve these roles, the arrangement of the IM-3 collagen fibers, their material properties, or both must accommodate the gradient of strain that is present in the mantle wall; during jet locomotion, the inner surface of the mantle may experience 1.5 times the circumferential strain of the outer surface during an escape jet (4). How can the IM-3

collagen fibers near the inner surface of the mantle wall accommodate greater strain, given the limited extensibility of squid mantle collagen (8, 10, 11)? For this initial analysis we focused on potential differences in the arrangement of the fibers that would allow the transmural strain gradient to be accommodated; the possibility of variation in the mechanical properties of the collagen fibers in IM-3 as a function of radial position has not yet been examined.

We used sonomicrometry to measure mantle kinematics during jetting in seven adult Atlantic longfin squid, *Doryteuthis pealeii* (Lesueur, 1821). We anesthetized each squid in cold seawater (12), then sutured two 1-mm-diameter sonomicrometry crystals (Sonometrics Corp., London, ON, Canada) to the outer surface of the mantle. One crystal was attached to the dorsal midline and one to the ventral midline; both were aligned in a transverse plane at a location one-third of the dorsal mantle length posterior to the anterior margin of the mantle (Fig. 1B), which is the region of the mantle that experiences the largest changes in diameter during jetting.

The animals were then placed in a narrow tank ($1.3 \times 0.3 \times 0.3$ m deep) filled with natural seawater at 17 °C. All animals recovered quickly and jetted as we acquired sonomicrometry data at 150 Hz. We startled the animals to elicit large amplitude hyper-inflations and escape jets, so that we measured maximal changes in the diameter of the outer surface of the mantle. We calculated circumferential strain (ϵ) at the outer surface of the mantle as follows:

$$\epsilon = \frac{D_I - D_R}{D_R}$$

where D_I was the instantaneous diameter of the outer surface of the mantle and D_R was the “resting” diameter of the outer surface of the mantle. D_R was defined as the mean maximum diameter of the outer surface of the mantle during respiratory movements of the mantle (dashed line in Fig. 3A). The value is simple to determine from sonomicrometry data and is similar to the diameter of the outer surface of the mantle in anesthetized animals (4).

Following the sonomicrometry experiments, the animals were anesthetized in cold seawater until quiescent, then decapitated. From each specimen two rings of mantle tissue (*i* and *ii* in Fig. 1B) were removed on each side of the transverse plane formed by the sonomicrometry crystals. One ring was stretched over a cork so that its diameter matched that of the maximum hyper-inflation recorded and was then pinned in place prior to being immersed in 10% formalin in seawater. The second ring was placed directly in the formalin solution, which typically causes contraction (Fig. 2A). After 24 hours in the fixative, the rings were transferred to 70% ethanol.

A small block of tissue was dissected from the ventral midline of the hyper-inflated and contracted mantle rings from each of the seven squid, yielding 14 tissue samples: one hyper-inflated block and one contracted block per squid. The tissue blocks were embedded in glycol methacrylate plastic (Technovit 7100, Heraeus Kulzer GmbH, Wehrheim, Germany), sectioned at 5–7 μm with glass knives, and stained using the Picosirius method (13).

We employed a dimensionless “waviness index” (14, 15) to quantify the folding of IM-3 collagen fibers and to

document potential transmural variation in folding. The waviness index was defined here as the ratio of the total length of the folded fiber to the straight-line distance between two ends of the fiber. A waviness index of 1.0 is obtained for a straight fiber, and the index increases with increasing folding.

We measured the waviness index for IM-3 collagen fibers sampled from near the outer surface of the mantle wall and from near the inner lumen surface (in a zone about 10% of the mantle thickness for each) for both contracted and hyper-inflated mantle tissue (Fig. 2B, C). For each location, we averaged the waviness indices of 15 fibers to determine the mean waviness index of that region. These measurements yielded a mean waviness index for inner and outer mantle IM-3 fibers in both hyper-inflated and contracted tissue for each squid. We then performed paired Student’s *t*-tests to compare the average waviness index of inner and outer fibers for the hyper-inflated samples and also for the contracted samples.

During escape jets, the mean circumferential strain measured during hyper-inflation was $+0.10 \pm 0.02$ (mean \pm s.d.) and during contraction was -0.31 ± 0.04 (Fig. 3A).

In tissue samples in the hyper-inflated state, IM-3 collagen fibers were observed to be essentially straight (Fig. 2B), and there were no significant differences in the mean (\pm s.d.) waviness index between the fibers from near the outer (1.034 ± 0.027 , $n = 7$) and inner (1.038 ± 0.035 , $n = 7$) surfaces of the mantle wall ($P = 0.37$; Fig. 3B). In the contracted state (Fig. 2C), however, the IM-3 fibers from near the inner surface of the mantle wall were significantly more folded (1.48 ± 0.14 , $n = 7$) than fibers from near the outer surface (1.32 ± 0.11 , $n = 7$) ($P < 0.01$; Fig. 3B).

Our results suggest that the connective tissue fibers in IM-3 are arranged to accommodate the nonuniformity in circumferential strain present in the mantle wall. Because the IM-3 collagen fibers near the inner surface of the contracted mantle show a higher waviness index compared with those near the outer surface, expansion of the mantle can produce greater strain in the mantle tissue near the inner lumen before the IM-3 fibers in this region are fully straightened. Although we did not measure the waviness index of fibers through the entire thickness of the mantle wall, our results imply that there is a gradient in the waviness index between the inner and outer surface of the mantle in the contracted state. In the hyper-inflated mantle samples the fibers were unfolded, with a mean waviness index just above 1.0 for both the outer and inner surfaces of the mantle wall, and with no statistically significant difference in the waviness index. It is unclear if the small amount of waviness still visible in some of the fibers in the expanded mantle (Figs. 2B, 3B) is an artefact of the shrinkage that is common in tissue processed for histology or if it represents the actual state of the fibers. We attempted to minimize shrinkage by using glycol methacrylate methods that are

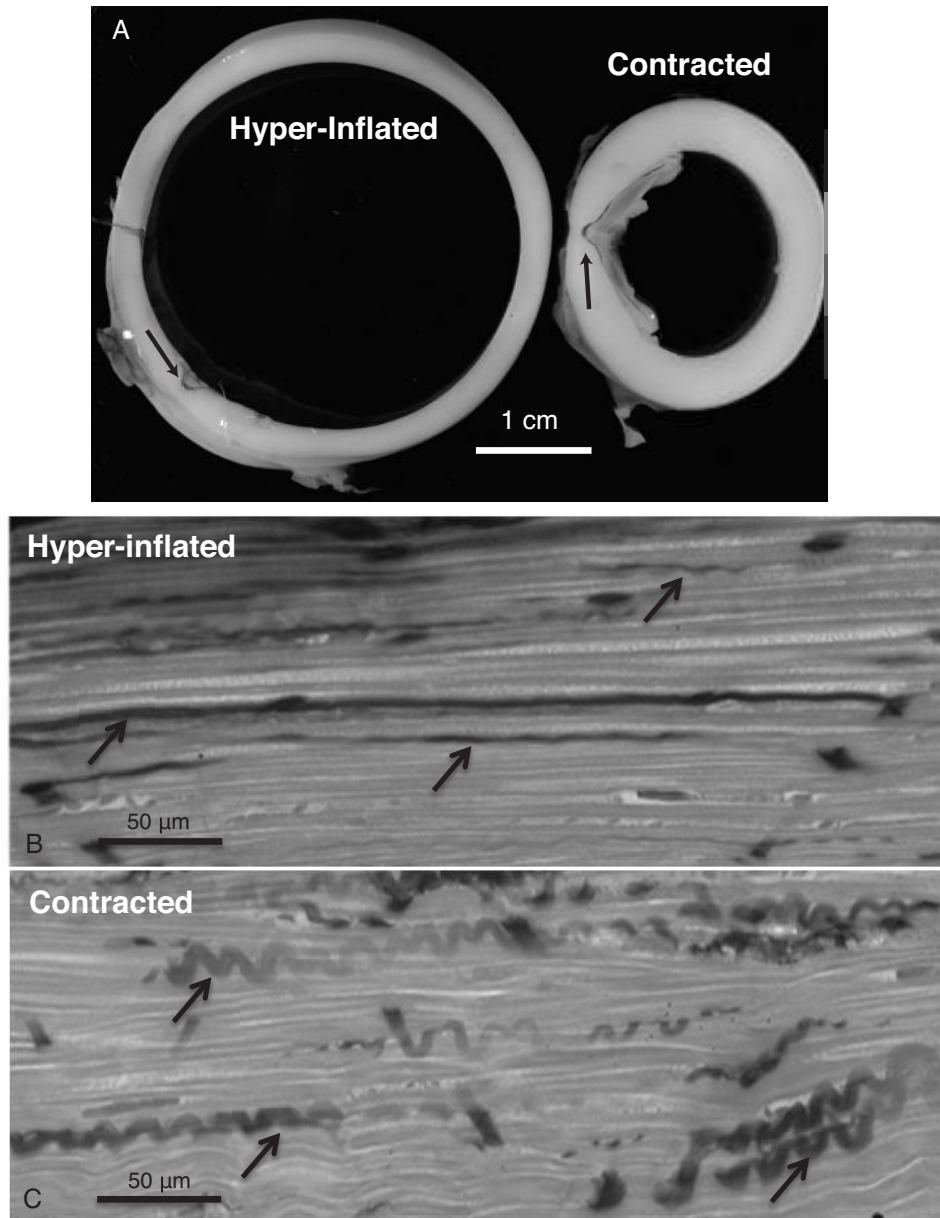


Figure 2. Photograph (A) and photomicrographs (B, C) of the hyper-inflated and contracted states. Arrows in A indicate the gladius, or pen; arrows in B and C indicate several IM-3 fibers.

superior in this regard to normal histological processing in paraffin.

The presence of some waviness, however, does not necessarily indicate that the fibers are unstrained. To demonstrate this, we first used the waviness index in the contracted state for each squid and calculated (see Fig. 3 caption for details) the mantle circumference at which the waviness index should be 1.0, and then compared that value to the measured hyper-inflated circumference. In all cases the measured hyper-inflated circumference was greater than the circumference required to straighten the IM-3 fibers fully (Fig. 3C), thus suggesting that even folded fibers experience

tensile strain. In other words, a typical hyper-inflation should be more than sufficient to straighten the IM-3 collagen fibers completely, yet the fibers remained slightly wavy. The ability of a hyper-inflated mantle to spring back to its resting diameter in the absence of circular muscle activity (9) suggests that the IM-3 fibers store elastic energy even if not straightened completely. Analogously, research on the elastic lamellae of porcine aorta wall showed that the lamellae were under significant tensile strain, even though they exhibited folding (15).

Interestingly, our calculations of the strain experienced by the IM-3 fibers during hyper-inflation (Fig. 3C) suggest

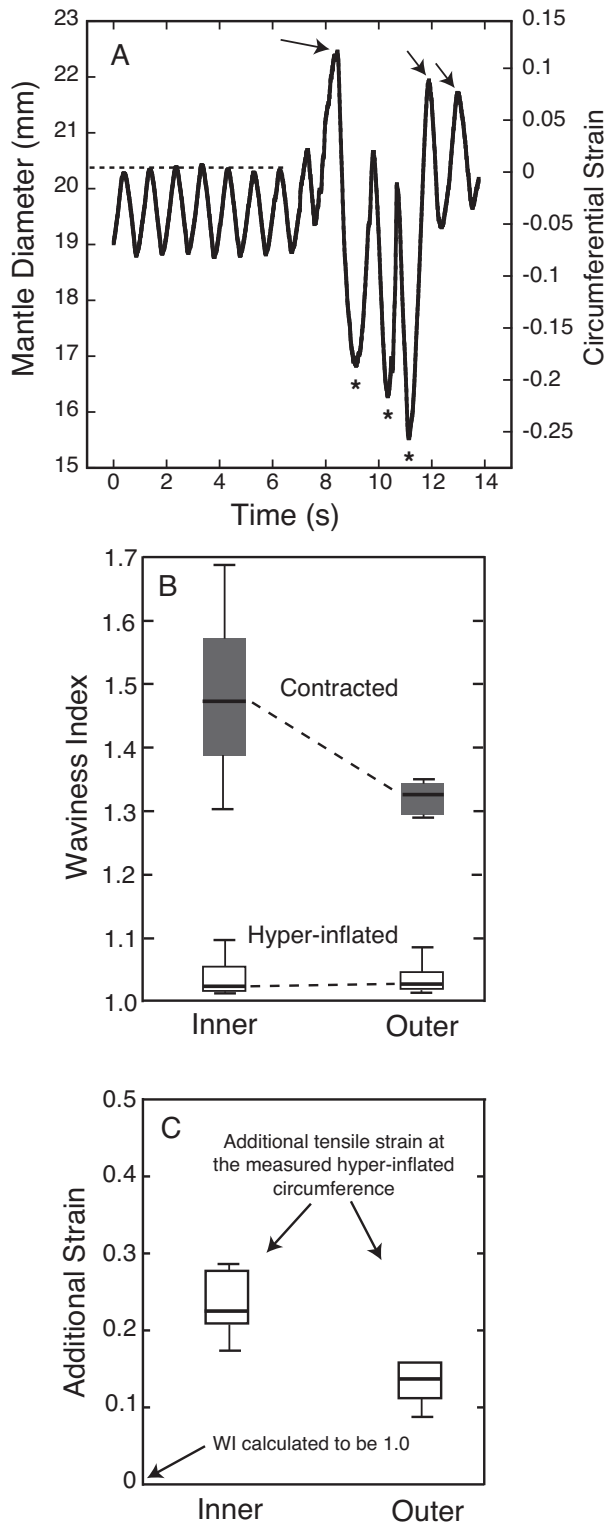


Figure 3. (A) Sonomicrometry data from one squid showing mantle diameter changes (left vertical axis) and circumferential strains at the outer surface of the mantle (right vertical axis) for a series of ventilatory jets followed by three escape jets (*). Arrows show hyper-inflations. Negative circumferential strains indicate mantle contractions relative to the mantle at rest (dashed line); positive strains indicate hyper-inflations. (B) Box plot

that those fibers need to accommodate greater tensile strain than is typical for collagen. Because we do not know if the fibers are continuous around the circumference, or how they are anchored or interconnected, there may be other components in the mantle wall in series that are strained. In addition, the calculations suggest that the additional strain at the inner surface of the mantle is higher than that at the outer surface. This result should be viewed with caution since the calculations of additional strain overestimate the additional strain in the inner fibers and underestimate the additional strain in the outer fibers. This is because the inner IM-3 fibers measured were in a zone adjacent to the inner surface that was about 10% of the mantle thickness and thus were subject to smaller strain than the inner surface itself. Likewise, the outer IM-3 fibers measured were in a zone adjacent to the outer surface that was about 10% of the mantle thickness and thus were subject to greater strain than the outer surface.

The morphological variation in collagen fiber organization we report here thus appears to allow the IM-3 fibers throughout the mantle wall to all be strained similarly at the peak of mantle hyper-inflation, thereby allowing all fibers to contribute to limiting mantle expansion and storing elastic energy. The results we present do not exclude the possibility that the IM-3 collagen fibers near the inner surface of the mantle wall have different mechanical properties than those near the outer surface. Although additional experiments are required to explore transmural differences in those properties, it is worth noting that at least two biochemically distinct types of collagen are present in the mantle and arms of some cephalopods (16, 17).

Transmural gradients of circumferential strain increase in magnitude as the relative thickness of the mantle wall increases (4). Hence, we predict that the proportionately thin mantle walls of newly hatched squid exhibit a smaller transmural difference in waviness index in the contracted state than those in the adult squid we examined. How IM-3 collagen fibers are laid down during development and then modified to accommodate the predicted ontogenetic change in transmural circumferential strain is unknown but represents an intriguing area for future study.

These results have implications for reinforcement of the

illustrating the effects of position and state of contraction on waviness index. (C) Prediction of additional tensile strain in the mantle in the hyper-inflated state after the waviness index (WI) was calculated to be 1.0. To make the predictions, we multiplied the circumference (measured from photographs like those in Fig. 2A) of the inner or outer surface of the mantle in the contracted state by the appropriate WI in the contracted state to predict the hyper-inflated circumference at which $WI = 1.0$. The additional tensile strain was then calculated as $(C_{Meas} - C_{Pred})/C_{Pred}$, where C_{Meas} was the measured circumference of the hyper-inflated mantle and C_{Pred} was the predicted circumferences of the mantle at which $WI = 1.0$. For B and C, the boxes represent the upper and lower quartiles; the whiskers extend 1.5 times the interquartile range; the bar represents the median.

connective tissue fibers in any cylindrical body wall or organ that undergoes changes in diameter. For example, the waviness index of the elastic lamellae of the thoracic aorta of pigs shows a pattern similar to that of the collagen fibers of the mantle, with the highest index observed near the inner wall and the lowest index near the outer wall (15). As in the squid mantle, such an arrangement may provide a means to equalize the strain in the lamellae in spite of the nonuniform circumferential strain that occurs as the aorta expands in diameter. Moreover, the orientation of collagen fibers has been shown to vary transmurally in human brain arteries in response to the stress distribution in the vessel wall (18, 19). It would be of interest to examine potential transmural differences in fiber waviness or crimping in these vessels as well. Finally, we hypothesize that variation in waviness index may be a common but unrecognized response to transmural gradients of strain in the hollow, cylindrical body walls of other invertebrates.

Acknowledgments

We thank Dr. Jack Weiss for assistance with the statistical analyses. Financial support was provided by National Science Foundation grants IOS-0950827 to JTT and IOS-0951067 to WMK.

Literature Cited

1. Clark, R. B. 1964. *Dynamics in Metazoan Evolution*. Clarendon Press, Oxford.
2. Wainwright, S. A. 1988. *Axis and Circumference: The Cylindrical Shape of Plants and Animals*. Harvard University Press, Cambridge, MA.
3. Lin, H. T., D. J. Slate, C. R. Paetsch, A. L. Dorfmann, and B. A. Trimmer. 2011. Scaling of caterpillar body properties and its biomechanical implications for the use of a hydrostatic skeleton. *J. Exp. Biol.* **214**: 1194–1204.
4. Thompson, J. T., K. R. Taylor, and C. Gentile. 2010. Gradients of strain and strain rate in the hollow muscular organs of soft-bodied animals. *Biol. Lett.* **6**: 482–485.
5. Thompson, J. T., J. A. Szczepanski, and J. Brody. 2008. Mechanical specialization of the obliquely striated circular mantle muscle fibres of the long-finned squid *Doryteuthis pealeii*. *J. Exp. Biol.* **211**: 1463–1474.
6. Bone, Q., A. Pulsford, and A. D. Chubb. 1981. Squid mantle muscle. *J. Mar. Biol. Assoc. UK* **61**: 327–342.
7. Gosline, J. M., and R. E. Shadwick. 1983. Molluscan collagen and its mechanical organization in squid mantle. Pp. 371–398 in *The Mollusca, Metabolic Biochemistry and Molecular Biomechanics*, Vol. 1, P. W. Hochachka, ed. Academic Press, New York.
8. Gosline, J. M., and R. E. Shadwick. 1983. The role of elastic energy storage mechanisms in swimming: an analysis of mantle elasticity in escape jetting in the squid, *Loligo opalescens*. *Can. J. Zool.* **61**: 1421–1431.
9. Gosline, J. M., J. D. Steeves, A. D. Harman, and M. E. DeMont. 1983. Patterns of circular and radial mantle muscle activity in respiration and jetting of the squid *Loligo opalescens*. *J. Exp. Biol.* **104**: 97–109.
10. MacGillivray, P. S., E. J. Anderson, G. M. Wright, and M. E. DeMont. 1999. Structure and mechanics of the squid mantle. *J. Exp. Biol.* **202**: 683–695.
11. Curtin, N. A., R. C. Woledge, and Q. Bone. 2000. Energy storage by passive elastic structures in the mantle of *Sepia officinalis*. *J. Exp. Biol.* **203**: 869–878.
12. O'Dor, R. K., and R. E. Shadwick. 1989. Squid, the olympian cephalopods. *J. Cephalopod Biol.* **1**: 33–55.
13. Cerri, P. S., and E. Sasso-Cerri. 2003. Staining methods applied to glycol methacrylate embedded tissue sections. *Micron* **34**: 365–372.
14. Wolinsky, H., and S. Glagov. 1964. Structural basis for the static mechanical properties of the aortic media. *Circ. Res.* **14**: 400–413.
15. Lillie, M. A., and J. M. Gosline. 2006. Tensile residual strains on the elastic lamellae along the porcine thoracic aorta. *J. Vasc. Res.* **43**: 587–601.
16. Morales, J., P. Montero, and A. Moral. 2000. Isolation and partial characterization of two types of muscle collagen in some cephalopods. *J. Agric. Food Chem.* **48**: 2142–2148.
17. Torres-Arreola, W., R. Pacheco-Aguilar, R. R. Sotelo-Mundo, O. Rouzaud-Sánchez, and J. M. Ezquerro-Brauer. 2008. Caracterización parcial del colágeno extraído a partir del manto, aleta y tentáculos de calamar gigante (*Dosidicus gigas*). *Cienc. Tecnol. Alimentaria* **6**: 101–108.
18. Finlay, H. M., L. McCullough, and P. B. Canham. 1995. Three-dimensional collagen organization of human brain arteries at different transmural pressures. *J. Vasc. Res.* **32**: 301–312.
19. Driessen, J. B., W. Wilson, C. V. C. Bouten, and F. P. T. Baaijens. 2004. A computational model for collagen fibre re-modelling in the arterial wall. *J. Theor. Biol.* **226**: 53–64.